

## OPEN ACCESS

EDITED BY  
Riccardo Bartoletti,  
University of Pisa, Italy

REVIEWED BY  
Yuan Zhang,  
Guangzhou Medical University, China  
Pinuccia Faviana,  
University of Pisa, Italy

\*CORRESPONDENCE  
Pengfei Liu  
✉ snowlpr@163.com

SPECIALTY SECTION  
This article was submitted to  
Genitourinary Oncology,  
a section of the journal  
Frontiers in Oncology

RECEIVED 19 October 2022  
ACCEPTED 23 January 2023  
PUBLISHED 02 February 2023

CITATION  
Sun X and Liu P (2023) Prognostic  
biomarker NEIL3 and its association  
with immune infiltration in renal clear  
cell carcinoma.  
*Front. Oncol.* 13:1073941.  
doi: 10.3389/fonc.2023.1073941

COPYRIGHT  
© 2023 Sun and Liu. This is an open-access  
article distributed under the terms of the  
[Creative Commons Attribution License  
\(CC BY\)](https://creativecommons.org/licenses/by/4.0/). The use, distribution or  
reproduction in other forums is permitted,  
provided the original author(s) and the  
copyright owner(s) are credited and that  
the original publication in this journal is  
cited, in accordance with accepted  
academic practice. No use, distribution or  
reproduction is permitted which does not  
comply with these terms.

# Prognostic biomarker NEIL3 and its association with immune infiltration in renal clear cell carcinoma

Xiaomei Sun<sup>1</sup> and Pengfei Liu<sup>2\*</sup>

<sup>1</sup>Graduate School, Tianjin University of Traditional Chinese Medicine, Tianjin, China, <sup>2</sup>Department of Medical Oncology, Tianjin Academy of Traditional Chinese Medicine Affiliated Hospital, Tianjin, China

**Background:** Kidney renal clear cell carcinoma (KIRC) is a malignant tumor with a high degree of immune infiltration. Identifying immune biomarkers is essential for the treatment of KIRC. Studies have identified the potential of NEIL3 to modulate the immune microenvironment and promote tumor progression. However, the role of NEIL3 in KIRC remains uncertain. This study was to investigate the effect of NEIL3 on the prognosis and immune infiltration of patients with KIRC.

**Methods:** TCGA and GEO databases were used to study the expression of NEIL3 in KIRC. Cox regression analysis was used to examine the relationship between the expression of NEIL3 and clinicopathological variables and survival. Furthermore, Gene Set Cancer Analysis (GSCA) was applied to study the impact of NEIL3 methylation on outcomes of KIRC. Through gene ontology (GO) and Gene set enrichment (GSEA) analysis, the biological processes and signal pathways related to NEIL3 expression were identified. In addition, immune infiltration analysis was conducted via CIBERSORT analysis, ssGSEA analysis and TISIDB database.

**Results:** NEIL3 was overexpressed in KIRC, and it was significantly related with histologic grade, pathologic stage, T stage, M stage, and vital status of KIRC patients ( $P < 0.001$ ). The expression of NEIL3 was associated with worse outcomes. Univariate and multivariate Cox analysis showed that NEIL3 may be an indicator of adverse outcomes in KIRC. GSEA analysis revealed that NEIL3 may be involved in signal pathways including cell cycle, DNA replication, mismatch repair, P53 signal pathway, and antigen processing and presentation. In addition, immune infiltration analysis showed a positive correlation between NEIL3 expression and multiple immune cells (activated CD8 T cells, activated dendritic cells, myeloid-derived suppressor cells, follicular helper T cells, and regulatory T cells) and immunoinhibitors (PD1, CTLA4, LAG3, TIGIT, IL10, and CD96).

**Conclusion:** NEIL3 is a potential independent biomarker of KIRC, which is relevant to immune infiltration.

## KEYWORDS

NEIL3, biomarker, kidney renal clear cell carcinoma, immune infiltration, prognosis

## Introduction

Renal cell carcinoma (RCC) is a common malignancy and accounts for more than 90% of kidney tumors, of which kidney renal clear cell carcinoma (KIRC) is the most prevalent, accounting for about 60%-85% of kidney cancers (1). According to epidemiological statistics, RCC accounts for 2% of cancer-related diagnoses and deaths worldwide, and the incidence of RCC has continued to increase in most countries and regions over the past few decades (2, 3). With the rapid development of targeted therapy and immunotherapy in the past decade, the 5-year survival rate of RCC patients, especially those with early local lesions, has improved significantly, but the overall prognosis remains poor (4, 5). In addition, the widespread use of targeted drugs and immunological agents has inevitably led to drug resistance problems (6). Therefore, it is essential to develop some effective biomarkers to assess the prognosis of patients and their response to treatment.

Endonuclease VIII-like 3 (NEIL3) is a monofunctional glycosylase involved in DNA interstrand crosslink damage repair and has an important role in maintaining telomere integrity (7, 8). Previous studies have shown that NEIL3 can repair oxidative telomere damage during the S phase, and deletion of NEIL3 can lead to telomere fusion, translocation, and loss, which indicates that NEIL3 serves a pivotal role in DNA repair (9). NEIL3 deficiency is also associated with increased lymphocyte apoptosis and autoimmune susceptibility (10). A study has found that NEIL3 can prevent senescence in hepatocellular carcinoma by repairing oxidative damage to telomeres during mitosis, and it is associated with poor prognosis (11). The overexpression of NEIL3 is also related to metastasis and poor prognosis in melanoma patients (12). In addition, there is evidence that NEIL3 is correlated with astrocytoma progression, drug resistance, and survival prognosis (13). However, the impact of NEIL3 on the prognosis and immunotherapy in patients with KIRC is poorly understood.

In this study, we investigated the relationship between NEIL3 expression and clinical features and outcomes of KIRC patients. Then, we explored the potential biofunctions of NEIL3 through GO analysis, and identified the carcinogenic and immune-related pathways using GSEA analysis. In addition, we investigated the impact of NEIL3 methylation on survival in KIRC patients. Finally, we also evaluated the connection between NEIL3 and immune infiltration levels and immunomodulators.

## Materials and methods

### Data source and preprocessing

Firstly, the expression level of NEIL3 in pan-cancer, including KIRC, was investigated by using the Tumor Immune Estimation Resource (TIMER.0) database (<http://timer.cistrome.org/>) (14). Level 3 RNA-sequencing data (HTSeq-Counts and HTSeq-FPKM) and clinical information of KIRC were downloaded from the UCSC Xena browser (<https://xenabrowser.net/>) (15). We converted HTSeq-FPKM data into transcripts per million (TPM) format for further analyses, and used HTSeq-Counts for differential analysis by the DESeq2 package. Cases with complete clinical characteristics and survival information were included in the study.

Microarray data of KIRC expression profiling (GSE40435, GSE53757 (16), GSE68417 (17) and GSE73731) were obtained from Gene Expression Omnibus (GEO) database (<https://www.ncbi.nlm.nih.gov/geo/>) (18). All gene expression microarray data were normalized using the limma R package. GSE40435, GSE53757 and GSE68417 were used to validate the differential expression of NEIL3 in clear cell carcinoma and normal tissues. GSE73731 with 265 KIRC samples was used to verify the relationship between NEIL3 expression and immune infiltration.

### Survival analysis and prognostic model construction

Clinical parameters of KIRC patients, including age, sex, histological grade, pathological stage, TNM stage, and vital status, were selected from previously downloaded clinical information for further analysis. Subsequently, based on median NEIL3 expression, we classified the patients into two groups. The survival curves were plotted to compare overall survival (OS), progression-free interval (PFI), and disease-specific survival (DSS) between two groups by the R package *survminer* (19). The receiver operating characteristic (ROC) curve was drawn by the R package *pROC* to verify the diagnostic value of NEIL3. We identified risk factors by univariate and multivariate Cox analysis. Furthermore, we construct a nomogram model by using the R package *rms*. The calibration curves were plotted to compare the consistency of the model prediction probability with the observed probability. The time-dependent ROC was performed by using the *timeROC* package to evaluate the prediction accuracy of the model. Moreover, we performed a decision curve analysis (DCA) to verify the clinical value of the predictive model.

### Functional enrichment analysis

Gene Ontology (GO) analysis was performed to predict NEIL3-related biological functions using the R package *clusterProfiler* (20). GSEA v4.2.3 software (21) was used for gene set enrichment analysis (GSEA) to identify NEIL3-related signal pathways. For each analysis, we set up 1000 permutations. The normalized enrichment score (NES) and false discovery rate (FDR) were applied to select significant pathway enrichment.

### Co-expression network analysis

To further investigate the molecular mechanisms associated with NEIL3, we used the GEPIA browser (<http://gepia.cancer-pku.cn/>) (22) to identify co-expressed genes significantly associated with NEIL3. Subsequently, Spearman's correlation analysis was carried out on the co-expressed genes. Meanwhile, the correlation between co-expressed genes and NEIL3 was also validated in the TIMER2.0 database. In addition, a protein-protein interaction (PPI) network was established through the STRING database (<https://cn.string-db.org/>) (23).

## Methylation analysis

Gene Set Cancer Analysis (GSCA) (<http://bioinfo.life.hust.edu.cn/GSCA/#/>) is a comprehensive platform, which can provide methylation analysis (24). Thus, we used the data from GSCA online software to analyze the relationship between NEIL3 methylation and survival in KIRC patients.

## Immune infiltration analysis

CIBERSORT was applied to calculate the proportion of 22 immune cells in KIRC patients (25). We performed single-sample Gene Set Enrichment Analysis (ssGSEA) to evaluate the relationship between NEIL3 expression and 28 immune cells by the R package GSVA (26). In addition, in order to predict the response of KIRC patients to immunotherapy, we also used TISIDB database (<http://cis.hku.hk/TISIDB/>) (27) to analyze the correlation between NEIL3 expression and immunomodulators.

## Statistical analysis

All statistical analyses were performed by R (4.1.3). Chi-square or Fisher's exact test was used to compare the clinical characteristics between high expression group and low expression group. Spearman's coefficient was used for correlation analysis. The association between clinicopathological features and NEIL3 expression was analyzed using the Wilcoxon signed-rank sum test and logistic regression. In this study, all hypothetical tests were bilateral, and  $P < 0.05$  was considered to be statistically significant.

## Results

### The overexpression of NEIL3 in KIRC

Firstly, we assessed NEIL3 expression levels in different human tumors using the TIMER database. We found that NEIL3 was overexpressed in multiple tumors, including KIRC (Figure 1A). In

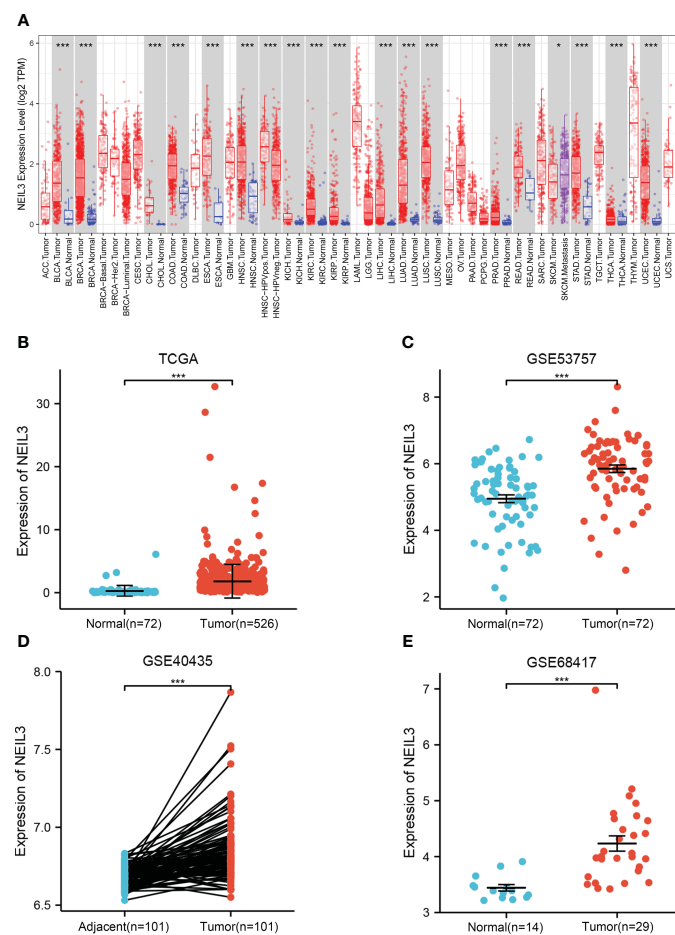


FIGURE 1

The expression level of NEIL3 is upregulated in KIRC. (A) Differential expression of NEIL3 between different tumors and adjacent normal tissues. NEIL3 is overexpressed in kidney renal clear cell carcinomas (KIRC), urothelial bladder carcinoma (BLCA), breast cancer (BRCA), colon adenocarcinoma (COAD), esophageal carcinoma (ESCA), liver hepatocellular carcinoma (LIHC), lung adenocarcinoma (LUAD). (B) NEIL3 expression level between tumor tissues and normal tissue in TCGA. (C–E) Comparison of NEIL3 expression level between tumor tissues and normal or adjacent tissues in the GSE53757 (C), GSE40435 (D), and GSE68417 (E) datasets. \*,  $P < 0.05$ ; \*\*\*,  $P < 0.001$ .

addition, we further evaluated the expression levels of NEIL3 in KIRC using TCGA and GEO data, and found that the NEIL3 expression level in KIRC tissues was remarkably higher compared with that in normal kidney tissues (all  $P < 0.001$ ) (Figures 1B–E).

## Association between NEIL3 expression and clinical features

To investigate the connection between clinical parameters and NEIL3 expression, our study incorporated clinical information of 539 KIRC samples from the TCGA database. Based on the median NEIL3 expression level, we divided these samples into two groups (low expression and high expression group). The results suggested that NEIL3 expression was closely related to histologic grade, pathologic stage, T stage, M stage, and vital status (all  $P < 0.001$ ) (Table 1). However, age ( $P = 0.698$ ), gender ( $P = 0.953$ ), and N stage ( $P = 0.062$ ) had no correlation with NEIL3 expression (Table 1).

## Prognostic analysis of NEIL3 in KIRC

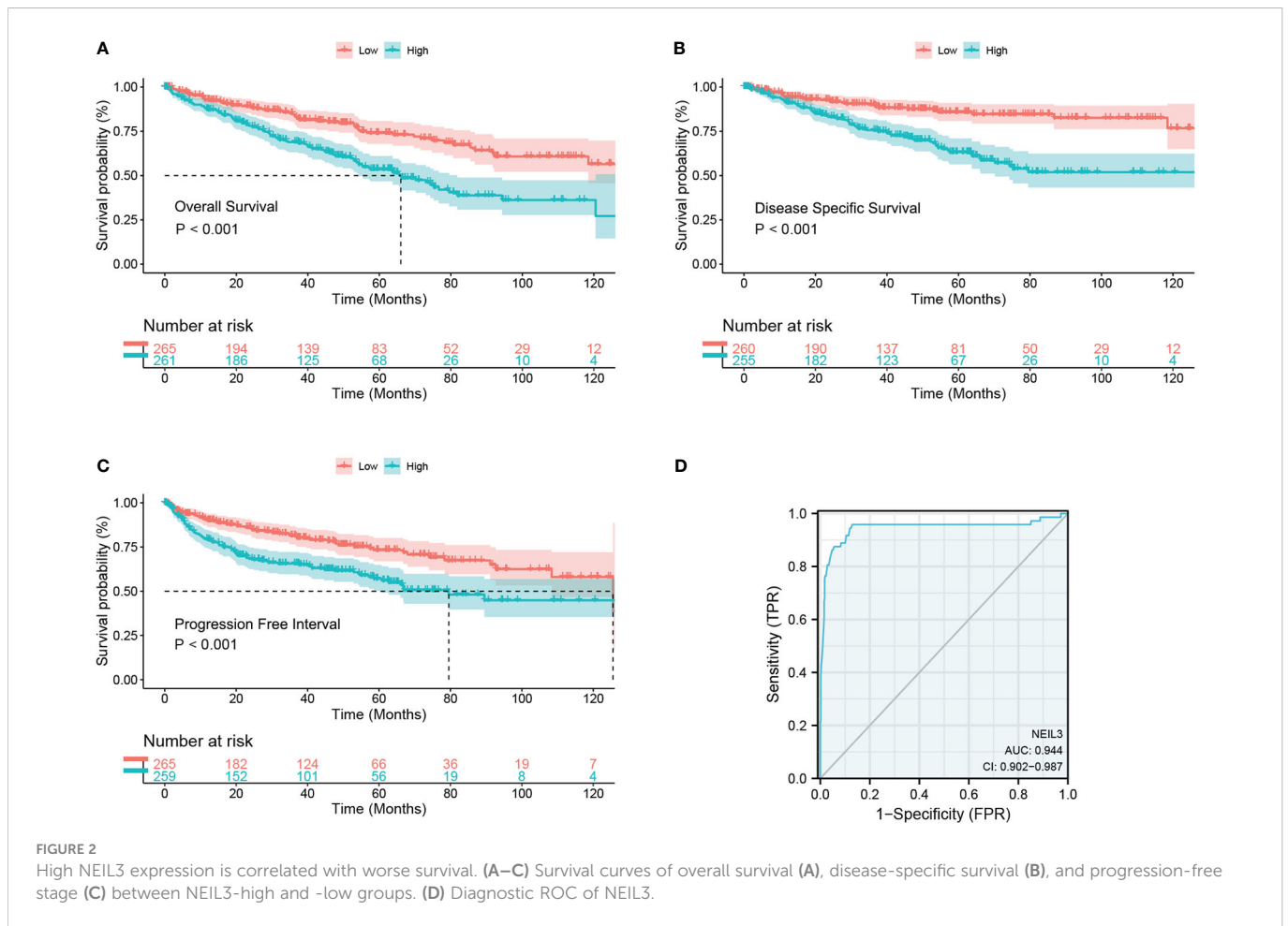
Survival analysis showed that up-regulation of NEIL3 was relevant to worse OS, DSS, and PFI in KIRC patients (Figures 2A–C). Moreover, we performed ROC analysis to assess the diagnostic value of NEIL3 to identify KIRC tissues, and found that the area under curve (AUC) value was 0.944 (Figure 2D). The result indicated that NEIL3 had a strong diagnostic performance. In addition, to further explore the risk factors for patients with KIRC, we conducted univariate and multivariate analyses. Univariate Cox regression analysis revealed that age, histologic grade, pathologic stage, TNM stage, and NEIL3 expression were associated with OS (Table 2). Multivariate Cox survival analysis showed that age ( $P = 0.046$ ), histologic grade, distant metastasis ( $P < 0.001$ ) and NEIL3 expression ( $P = 0.009$ ) were independent predictors of poor prognosis in KIRC patients (Table 2). Based on the multivariate cox regression analysis, a nomogram model was created to predict the probability of survival using NEIL3 expression levels, age, histologic grade, and M stage (Figure 3A). The calibration curves showed good agreement between the predicted OS and the observed OS at 1, 3, and 5 years (Figure 3B). The time ROC curve showed that the nomogram model could effectively predict the OS of KIRC patients at 1, 3, and 5 years (Figure 3C). Additionally, we obtained a consistency index (C-index) of 0.753. These results indicated that this model had a relatively reliable predictive performance.

In addition, we performed DCA analysis to verify the clinical practicability of the predictive model. The DCA curves revealed that the combined model had a higher net benefit in predicting OS at 1, 3, and 5 years compared to other models that included a single clinical variable (Figures 3D–F). The results indicated that the combination of NEIL3 with clinical features was beneficial to predict the prognosis of KIRC patients.

TABLE 1 Correlation between NEIL3 expression and clinicopathological variables in patients with KIRC.

Characteristic	Low expression of NEIL3	High expression of NEIL3	<i>P</i>
n	269	270	
Age, n (%)			0.698
<=60	137 (25.4%)	132 (24.5%)	
>60	132 (24.5%)	138 (25.6%)	
Gender, n (%)			0.953
Female	92 (17.1%)	94 (17.4%)	
Male	177 (32.8%)	176 (32.7%)	
Histologic grade, n (%)			< 0.001
G1	11 (2.1%)	3 (0.6%)	
G2	134 (25.2%)	101 (19%)	
G3	95 (17.9%)	112 (21.1%)	
G4	23 (4.3%)	52 (9.8%)	
Pathologic stage, n (%)			< 0.001
Stage I	157 (29.3%)	115 (21.5%)	
Stage II	33 (6.2%)	26 (4.9%)	
Stage III	54 (10.1%)	69 (12.9%)	
Stage IV	25 (4.7%)	57 (10.6%)	
T stage, n (%)			< 0.001
T1	160 (29.7%)	118 (21.9%)	
T2	39 (7.2%)	32 (5.9%)	
T3	69 (12.8%)	110 (20.4%)	
T4	1 (0.2%)	10 (1.9%)	
N stage, n (%)			0.062
N0	111 (43.2%)	130 (50.6%)	
N1	3 (1.2%)	13 (5.1%)	
M stage, n (%)			< 0.001
M0	225 (44.5%)	203 (40.1%)	
M1	23 (4.5%)	55 (10.9%)	
OS event, n (%)			< 0.001
Alive	205 (38%)	161 (29.9%)	
Dead	64 (11.9%)	109 (20.2%)	
Age, median (IQR)	60 (52, 69)	61 (52, 71)	0.715

$P < 0.05$ , statistically significant.



## Functional enrichment analysis of NEIL3

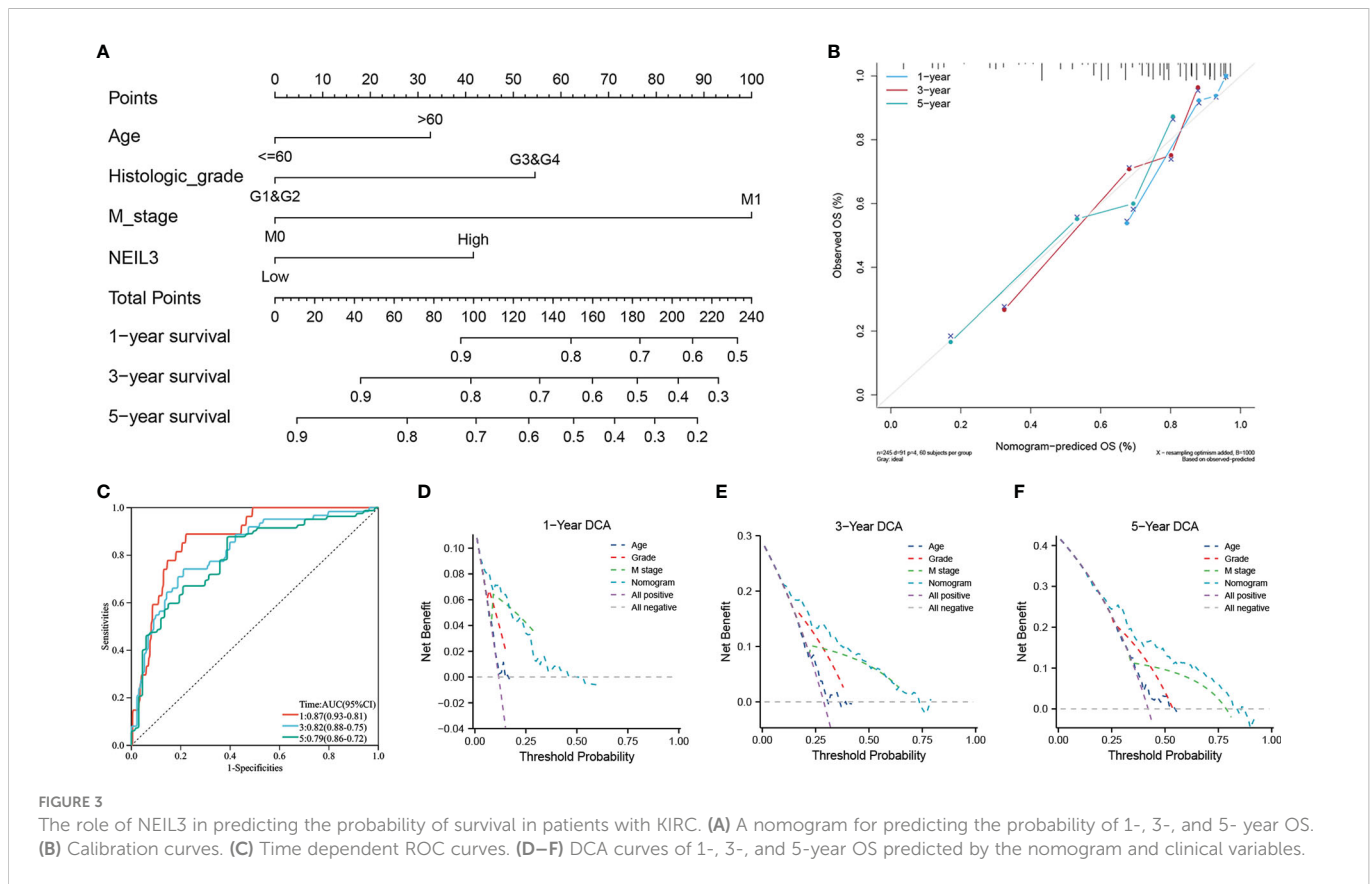
Next, we conducted a GO analysis to characterize the biological functions of NEIL3 in KIRC. The GO analysis showed that NEIL3 was engaged in multiple biological processes, including nuclear division, mitotic nuclear division, acute inflammatory response, kinetochore, chromosome condensation, serine hydrolase activity, and receptor-ligand activity signal pathway (Figure 4A). In addition, to further investigate NEIL3-related signal pathways in renal clear cell

carcinogenesis, we performed GSEA analysis and found 16 signal pathways demonstrated significant differences ( $NES > 1.72$ ,  $P$ -value  $< 0.05$ ,  $FDR < 0.1$ ) in the high expression group (Table 3). Cell cycle, DNA replication, mismatch repair, and p53 signal pathway are the important signal pathways involved in tumorigenesis in the high NEIL3 group, while the signal pathways involved in the immune response included antigen processing and presentation, intestinal immune network for IgA production, primary immunodeficiency (Figures 4B–H).

TABLE 2 Univariate analysis and multivariate analysis of the prognostic factors in KIRC patients.

Characteristics	HR (95%CI) Univariate analysis	<i>P</i> value Univariate analysis	HR (95%CI) Multivariate analysis	<i>P</i> value Multivariate analysis
Age (>60 vs. ≤60)	1.54 (1.01-2.36)	0.046	1.55 (1.01-2.39)	0.046
Gender (Male vs. Female)	1.05 (0.69-1.60)	0.833		
Grade (G3&G4 vs. G1&G2)	2.65 (1.66-4.23)	<0.001	1.72 (1.05-2.83)	0.032
Stage (III&IV vs. I&II)	3.48 (2.23-5.42)	<0.001	1.08 (0.42-2.77)	0.876
T stage (T3&T4 vs. T1&T2)	3.05 (2.00-4.66)	<0.001	1.87 (0.82-4.28)	0.138
N stage (N1 vs. N0)	3.09 (1.60-5.98)	0.001	1.50 (0.74-3.02)	0.259
M stage (M1 vs. M0)	4.11 (2.66-6.37)	<0.001	2.98 (1.75-5.09)	<0.001
NEIL3 (High vs. Low)	1.72 (1.13-2.63)	0.012	1.79 (1.16-2.77)	0.009

CI, confidence interval.  $P < 0.05$ , statistically significant.



## Analysis of genes coexpressed with NEIL3

In order to further explore the potential role of NEIL3 in renal clear cell carcinogenesis, we identified genes that were positively correlated with NEIL3 through the GEPIA database. The top ten related genes ( $r \geq 0.73$ ) are shown in the co-expression heatmap (Figure 5A). The interaction network for these genes was established by using the STRING database (Figure 5B). In addition, the correlation between NEIL3 and these genes was validated in the TIMER2.0 database. The analysis suggested that NEIL3 was significantly associated with KIFC1 ( $cor = 0.743$ ,  $P = 1.66e-94$ ), CDCA8 ( $cor = 0.79$ ,  $P = 8.04e-115$ ), TPX2 ( $cor = 0.786$ ,  $P = 4.1e-113$ ), ERCC6L ( $cor = 0.742$ ,  $P = 2.57e-94$ ), BIRC5 ( $cor = 0.726$ ,  $P = 1.7e-88$ ), KIF20A ( $cor = 0.731$ ,  $P = 4.4e-90$ ), GTSE1 ( $cor = 0.751$ ,  $P = 6.11e-98$ ), CENPA ( $cor = 0.781$ ,  $P = 8.46e-111$ ), ORC6 ( $cor = 0.653$ ,  $P = 4.54e-66$ ), AURKA ( $cor = 0.667$ ,  $P = 7.06e-70$ ) (Figures 5C–L).

## Association between NEIL3 methylation and prognosis of KIRC patients

Previous studies have illustrated that aberrant DNA methylation is closely related to the development and progression of multiple tumors (28, 29). In our study, we found that the methylation level of NEIL3 in renal clear carcinoma tissues was lower than that in normal renal tissues (Figure 6A). Spearman correlation analysis showed that there was a negative correlation between NEIL3 methylation and mRNA expression in KIRC ( $cor = -0.36$ ,  $FDR = 6e-11$ ) (Figure 6B). Furthermore, we found that compared with the hypermethylated

patients, NEIL3 hypomethylated patients had worse OS, progression-free survival (PFS) and DSS, while there was not significantly difference in disease-free interval (DFI) between the two groups (Figures 6C–F). Overall, patients with NEIL3 hypomethylation (indicating higher expression of NEIL3 mRNA) had worse survival outcomes than patients with NEIL3 hypermethylation.

## Relationship between NEIL3 expression and immune infiltration

In order to explore the association between NEIL3 expression and immune infiltration, we performed CIBERSORT and ssGSEA. CIBERSORT analysis showed that the proportion of plasma cells, T cells CD8, follicular helper T cells (Tfh), regulatory T cells (Tregs), and M0 macrophages was increased in the high expression group, whereas the fraction of resting NK cells, monocytes, and M2 macrophage was decreased in the high expression group (Figure 7A). Meanwhile, ssGSEA revealed that activated CD4 T cells, activated dendritic cells (DCs), activated CD8 T cells, macrophages, myeloid-derived suppressor cells (MDSCs), natural killer cells (NK cells), Tfh and Tregs were highly expressed in the NEIL3 overexpression group (Figure 7B). Furthermore, the connection between NEIL3 co-expressed genes and immune infiltration in KIRC was verified by ssGSEA. It was found that the expression levels of NEIL3 co-expressed genes had a positive association with multiple immune infiltrating cells (including B cells, CD4 T cells, CD8 T cells, DCs, MDSCs, Tfh, and Tregs, etc.) (Supplementary Figure 1).

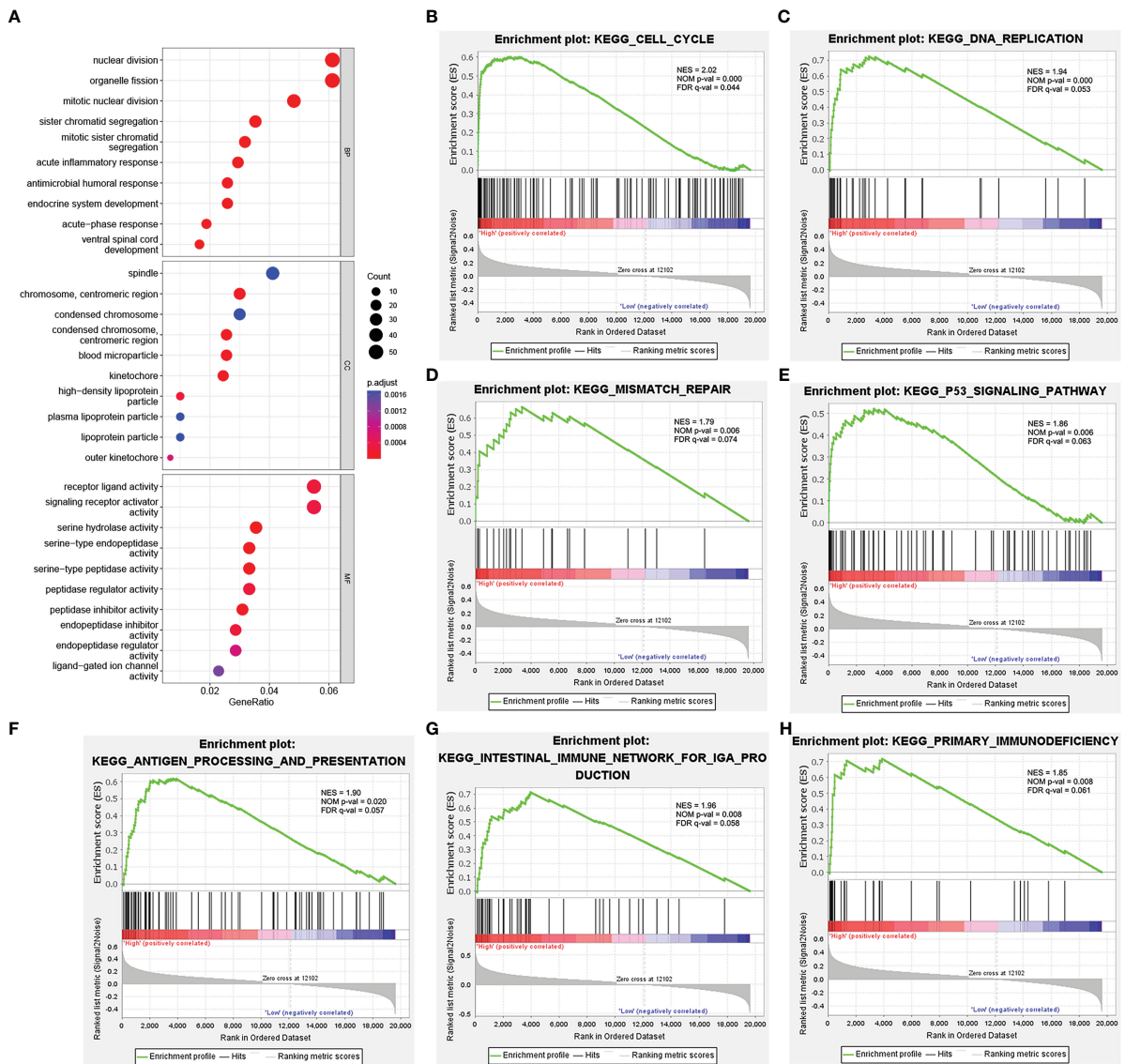


FIGURE 4

Functional enrichment analysis of NEIL3. (A) Enrichment plot from the GO analysis. Some biological processes (BP), cellular components (CC), and molecular functions (MF) were associated with NEIL3-related genes. (B–H) Enrichment plots from gene set enrichment analysis (GSEA). The GSEA results showed that the terms “Cell cycle”, “DNA replication”, “Mismatch repair”, “p53 signal pathway”, “Antigen processing and presentation”, “Intestinal immune network for IgA production”, and “Primary immunodeficiency” were differentially enriched in NEIL3 high expression phenotype. NES, normalized enrichment score; NOM p-value, nominal *P* value; FDR, false discovery rate.

We further verified the relation between the expression of tumor-infiltrating lymphocytes (TILs) and NEIL3 *via* the TISIDB database. The results indicated that the abundance of activated CD4 T cells ( $r = 0.668$ ,  $P < 2.2e-16$ ), activated CD8 T cells ( $r = 0.422$ ,  $P < 2.2e-16$ ), DCs ( $r = 0.4$ ,  $P < 2.2e-16$ ), MDSCs ( $r = 0.339$ ,  $P = 1.07e-15$ ), memory B cell ( $r = 0.358$ ,  $P = 8.74e-18$ ), Tfh cells ( $r = 0.332$ ,  $P = 4.84e-15$ ), NKT cells ( $r = 0.256$ ,  $P = 2.2e-09$ ), Type 1 T helper cell (Th1 cells) ( $r = 0.284$ ,  $P = 3.04e-11$ ), Type 2 T helper cell (Th2 cells) ( $r = 0.304$ ,  $P = 8.55e-13$ ) and Tregs ( $r = 0.231$ ,  $P = 7.12e-08$ ) was positively correlated with NEIL3 expression (Figures 8A–J). In addition, we divided 265 renal clear cell carcinoma samples from GSE73731 into two groups based on the median NEIL3 expression level. CIBERSORT and ssGSEA were used to assess the relationship between NEIL3 expression and the extent of immune infiltration. Similarly, we found a higher level of immune cell infiltration in the over expressed group (Supplementary Figure 2).

Overall, the high-expression group of NEIL3 had stronger immune infiltration than the low-expression group, especially regarding CD4 T cells, CD8 T cells, Tfh cells and Tregs.

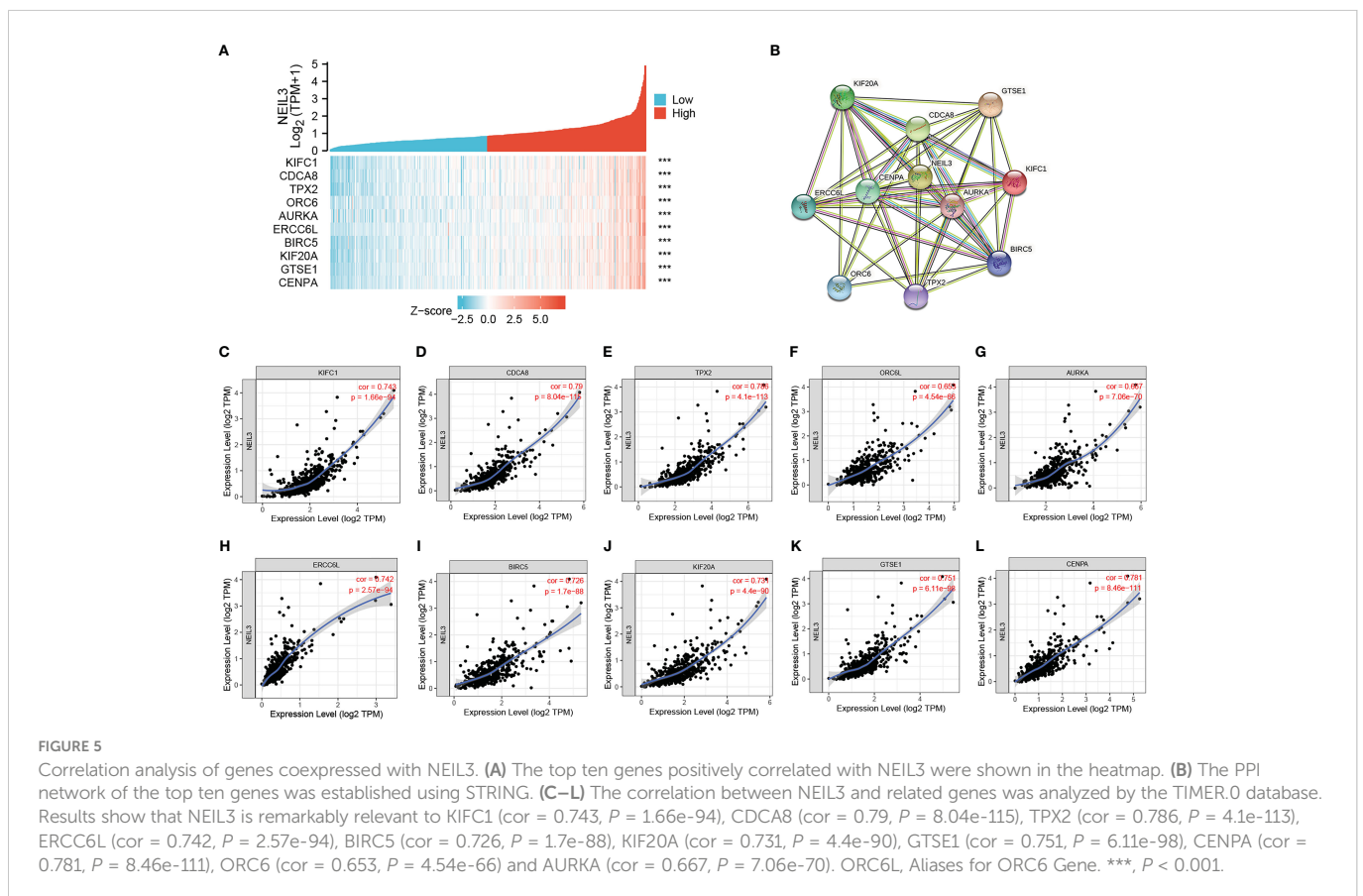
## Association between NEIL3 expression and immunoinhibitors

Finally, we investigated the association between 24 immunoinhibitors and NEIL3 expression using the TISIDB database. The heatmap showed that more than half of 24 immunoinhibitors were positively related to NEIL3 expression in KIRC (Figure 8K). Among them, the expression of PD1, CTLA4, LAG3, TIGIT, IL10, and CD96 was significantly associated with NEIL3 expression (all spearman's  $r \geq 0.3$ , all  $P < 0.001$ ) (Figures 8L–Q).

TABLE 3 Gene sets enriched in the high NEIL3 expression group.

GS follow link to MSigDB	SIZE	NES	NOM p-val	FDR q-val
KEGG_BASE_EXCISION_REPAIR	33	2.02	0.002	0.083
KEGG_CELL_CYCLE	124	2.02	0.000	0.044
KEGG_INTESTINAL_IMMUNE_NETWORK_FOR_IGA_PRODUCTION	46	1.96	0.008	0.058
KEGG_DNA_REPLICATION	36	1.94	0.000	0.053
KEGG_SYSTEMIC_LUPUS_ERYTHEMATOSUS	54	1.90	0.018	0.065
KEGG_ANTIGEN_PROCESSING_AND_PRESENTATION	80	1.90	0.020	0.057
KEGG_HOMOLOGOUS_RECOMBINATION	28	1.86	0.006	0.072
KEGG_P53_SIGNALING_PATHWAY	67	1.86	0.006	0.063
KEGG_PRIMARY_IMMUNODEFICIENCY	35	1.85	0.008	0.061
KEGG_AUTOIMMUNE_THYROID_DISEASE	50	1.83	0.015	0.063
KEGG_TYPE_I_DIABETES_MELLITUS	41	1.81	0.028	0.068
KEGG_PYRIMIDINE_METABOLISM	97	1.79	0.004	0.074
KEGG_MISMATCH_REPAIR	23	1.79	0.006	0.074
KEGG_VIRAL_MYOCARDITIS	68	1.77	0.026	0.079
KEGG_ALLOGRAFT_REJECTION	35	1.75	0.030	0.088
KEGG_LEISHMANIA_INFECTION	69	1.75	0.040	0.084

NES, normalized enrichment score; NOM, nominal; FDR, false discovery rate. Gene sets with NOM p-value < 0.05 and FDR q-value < 0.1 are considered as significant.



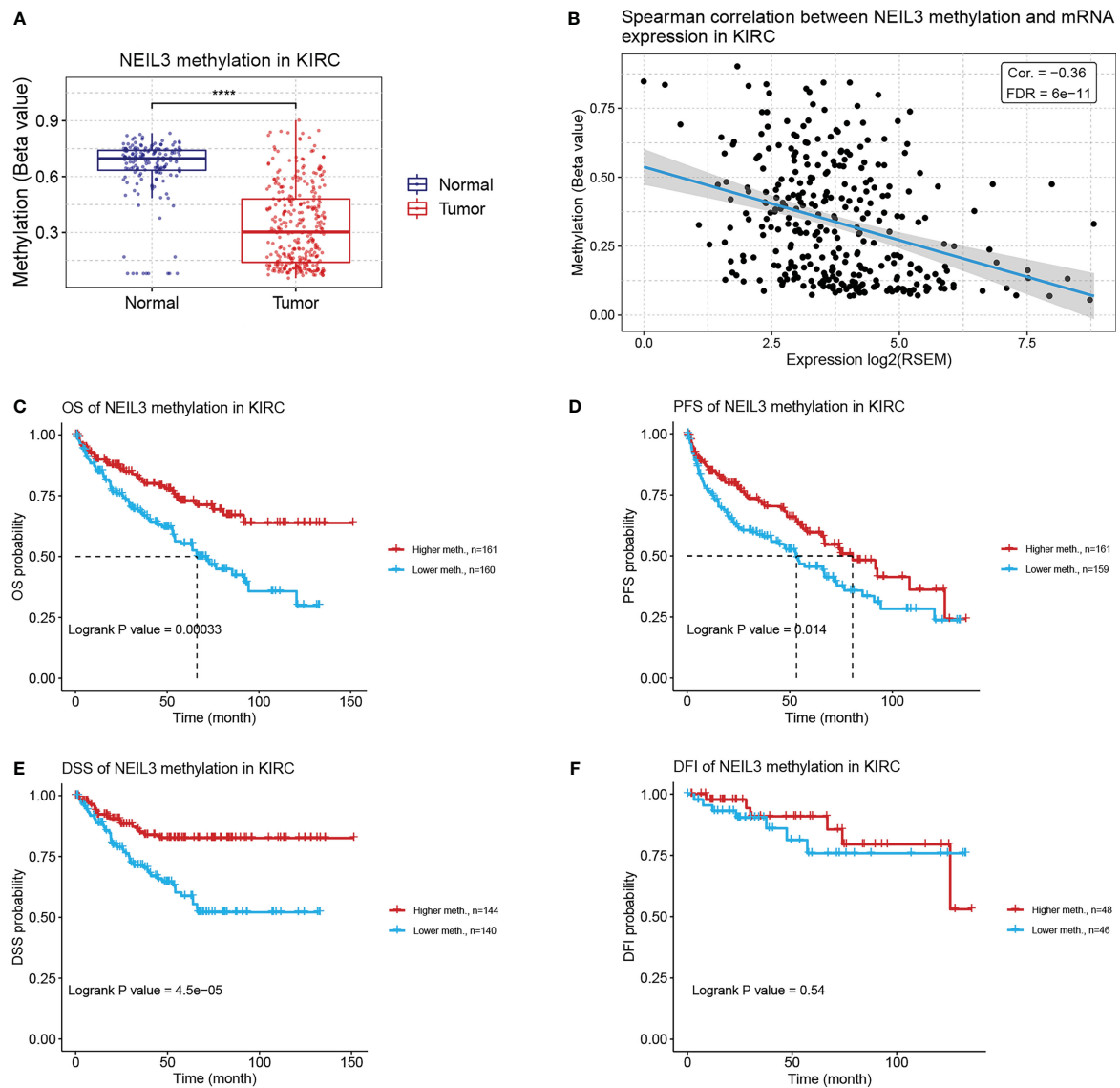


FIGURE 6

Correlation analysis between NEIL3 methylation and KIRC patients via the GSCA database. (A) The methylation level of NEIL3 between renal clear carcinoma tissues and normal renal tissues. (B) The correlation between NEIL3 methylation and mRNA expression. (C–F) The effect of NEIL3 methylation on overall survival (OS), progression-free survival (PFS), disease-specific survival (DSS), and disease-free interval (DFI) of patients with KIRC. \*\*\*\*,  $P < 0.0001$ .

## Discussion

This study revealed that the expression of NEIL3 was significantly increased in KIRC, and it was related to the histologic grade, pathologic stage, depth of invasion, distant metastasis, and vital status of KIRC patients, and that overexpression of NEIL3 was linked to worse OS, DSS, and PFI. Previous research has confirmed that NEIL3 has a crucial role in DNA repair (9), and it is related to adverse outcomes of several tumors, including hepatoma, lung cancer, and melanoma (11, 12, 30). In addition, our study showed that the increased expression of NEIL3 in KIRC tumors may be caused by its hypomethylation, and the OS, PFS, and DSS of NEIL3 hypomethylation patients are worse than those with hypermethylation patients. It has been confirmed that DNA methylation can modulate the transcription of oncogenes in human tumors (29). DNA methylation can serve as a biomarker for the

prognosis of common cancers (31), supporting our finding that KIRC patients with hypomethylated NEIL3 may have worse survival outcomes.

The GO analysis has indicated that NEIL3 is involved in mitotic nuclear division, acute inflammation, kinetochore and chromosome condensation, etc., and it has been proven that tumor cells can resist the attack of immune cells through higher expression of HLA-G and PD-L1 during mitosis, suggesting that the mitotic index has an essential impact on cancer immunotherapy (32). Acute inflammatory response can stimulate the maturation and antigen presentation of DCs, thus affecting the anti-tumor immune response (33). Furthermore, GSEA analysis has shown that NEIL3 is associated with multiple DNA damage repair pathways. It is known that DNA damage response involves DNA repair, cell cycle, replication stress response, and apoptosis mechanisms (34). Base excision repair, homologous recombination, and mismatch repair are three

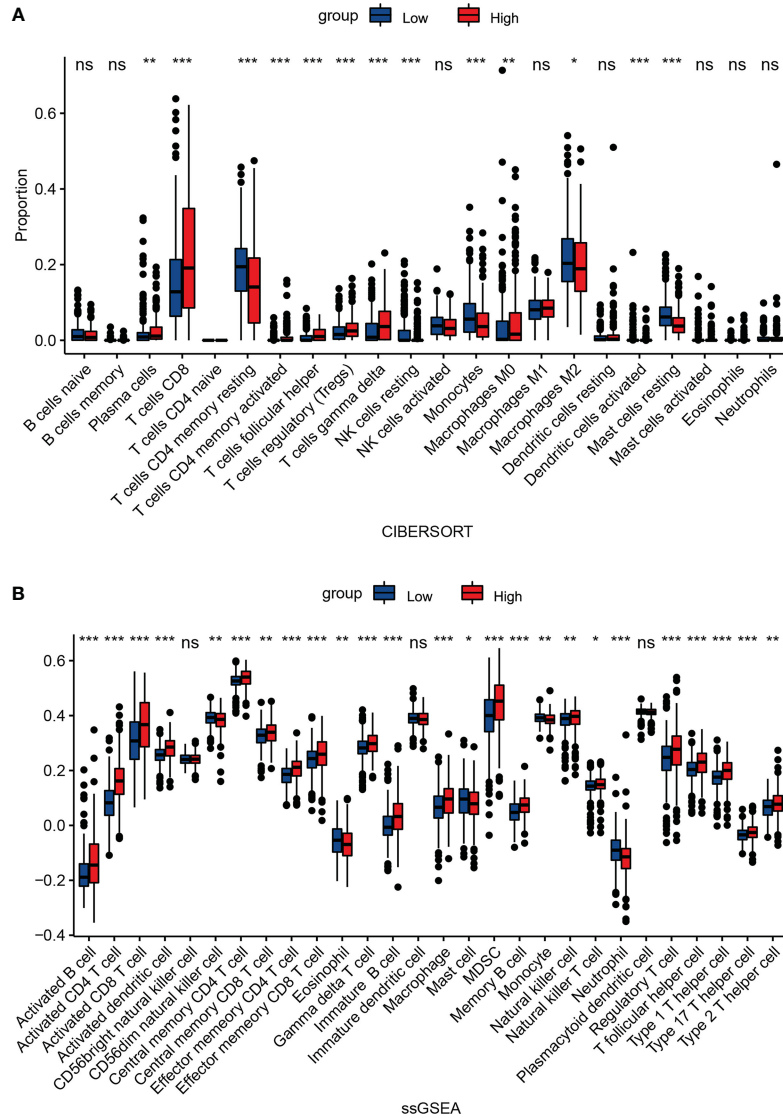


**FIGURE 7** Association between NEIL3 expression and immune infiltration level. Comparison of the proportion of 22 immune cells (A) and expression levels of 28 immune cells (B) between NEIL3-high and -low groups by CIBERSORT and ssGSEA, respectively. ns,  $P \geq 0.05$ ; \*,  $P < 0.05$ ; \*\*,  $P < 0.01$ ; \*\*\*,  $P < 0.001$ .

pathways of DNA damage repair. If the DNA damage response pathway is disrupted, it will increase the risk of cancer (34). For example, the mutations of BRCA gene can lead to homologous recombination defects, which can make cells more sensitive to ionizing radiation and chemical drugs, and increase the incidence of breast, ovarian and prostate cancer (35). Additionally, a recent study reported that mutant P53 can impair the innate immune response and promote the tumor microenvironment (36).

In addition, we identified immune-related signal pathways, including antigen processing and presentation, primary immunodeficiency, and intestinal immune network for IgA production. Tumor immune escape is closely related to the absence of antigen presentation mechanism caused by loss of HLA heterozygosity or  $\beta 2M$  mutation (37–39). HLA is primarily involved in the processing and presentation of tumor antigens, and it is essential for CD8+T cells to recognize tumors. McGranahan N has demonstrated that loss of HLA heterozygosity is a common immune escape mechanism in the evolution of lung cancer (37). A

study has shown that  $\beta 2M$  mutation can lead to the loss of expression of MHC I, and affect T cell recognition (39). It has been proved that the intestinal immune network producing IgA is essential in the occurrence of kidney carcinogenesis (40). Moreover, primary immunodeficiency may increase the risk of cancer development, especially lymphoma (41). Overall, NEIL3 is involved in diverse oncogenic and immunologically relevant biological processes and signal pathways and has the potential to be a promising target for KIRC.

In recent years, RCC has been regarded as a highly immunopermeable tumor, and studies have found that tumor immune infiltration is closely related to renal carcinogenesis (42, 43). There is increasing evidence that innate immune cells (macrophages, DCs, MDSCs, and NK cells) and adaptive immune cells (T and B cells) in the tumor microenvironment (TME) are closely linked to immune escape and tumor progression (44). Our results showed that the expression of NEIL3 was positively correlated with the abundance of T cells, macrophages, DCs, MDSCs, and NKT

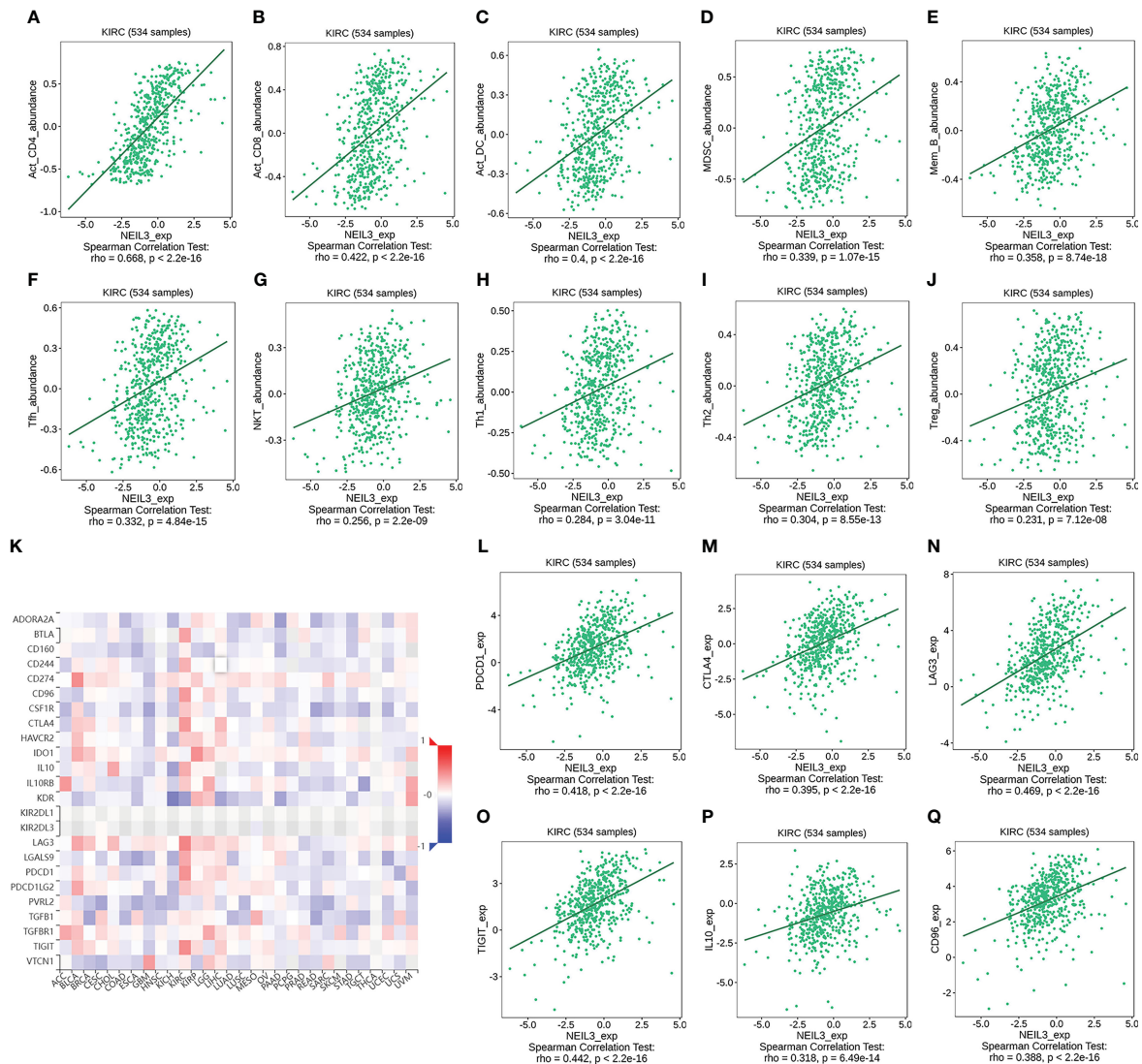


FIGURE 8

(A–J) Correlation analysis between the abundance of tumor-infiltrating lymphocytes (TILs) and NEIL3 expression using the TISIDB database. The results show that NEIL3 expression is positively correlated with activated CD4 T cells ( $r = 0.668$ ,  $P < 2.2e-16$ ), activated CD8 T cells ( $r = 0.422$ ,  $P < 2.2e-16$ ), activated dendritic cells (DCs) ( $r = 0.4$ ,  $P < 2.2e-16$ ), myeloid-derived suppressor cells (MDSCs) ( $r = 0.358$ ,  $P = 1.07e-15$ ), memory B cell ( $r = 0.358$ ,  $P = 8.74e-18$ ), follicular helper T cells (Tfh) ( $r = 0.332$ ,  $P = 4.84e-15$ ), NKT cells ( $r = 0.256$ ,  $P = 2.2e-09$ ), Type 1 T helper cell (Th1 cells) ( $r = 0.284$ ,  $P = 3.04e-11$ ), Type 2 T helper cells (Th2 cells) ( $r = 0.304$ ,  $P = 8.55e-13$ ) and regulatory T cells (Tregs) ( $r = 0.231$ ,  $P = 7.12e-08$ ). (K) The heatmap reveals the association between NEIL3 expression and 24 immunoinhibitors across multiple tumors. (L–Q) Scatterplots of the correlations between NEIL3 expression and immunomodulators of PDCD1, CTLA4, LAG3, TIGIT, IL10, and CD96 in KIRC are shown. PDCD1, Aliases for PD1 Gene.

cells. Previous studies have shown that KIRC is the tumor type with the highest infiltration of T cells, and the survival rate of KIRC subsets with the highest T-cell accumulation is the worst (45). In contrast to other carcinomas, in KIRC, it is reported that the infiltration level of CD8 T cells is associated with unfavorable outcomes (46, 47). In addition, high expression of Th2 cells and Tregs was shown to be associated with worse outcomes in KIRC patients (48). A previous study showed that B-lineage cells were associated with adverse outcomes and distant metastasis in KIRC (49). Current evidence has already shown that DCs can induce tumor immune surveillance and promote immune escape (50). MDSCs derived from myeloid progenitor cells can suppress the anti-tumor activity of T cells and NK cells, and promote immune escape. It can induce epithelial-mesenchymal transition (EMT), promote tumor progression and

metastasis, and promote angiogenesis (51). In addition, a meta-analysis has indicated that MDSCs are significantly correlated with poor outcomes of solid tumors, which has a good prognostic value (52).

Finally, we found that NEIL3 had positive connections with the expression of co-inhibitory molecules (such as PD1, CLTA-4, LAG-3, TIGIT, IL10, and CD96). Previous studies have shown that high expression of CTLA4, LAG3, and TIGIT is detrimental to the survival of KIRC patients (43). In addition, studies have identified the synergistic effect of LAG3 and PD1 in mediating T-cell exhaustion, thereby weakening anti-tumor activity (53). IL-10 is an immunosuppressive cytokine, which can promote T-cell exhaustion by regulating the expression of inhibitory receptors on TILs, thereby limiting effective anti-tumor immunity (54). Moreover, several

studies have found that increasing IL-10 expression levels correlate with poor outcomes in cancer patients (55). These results suggest that NEIL3 has the potential to modulate tumor immune microenvironment and promote KIRC progression, but its direct mechanism requires further investigation.

Conclusively, our findings suggest that NEIL3 is highly expressed in KIRC, and it is associated with a worse prognosis. Moreover, higher NEIL3 expression is connected with more extensive immune cell infiltration. Thus, NEIL3 might be a promising biomarker for KIRC.

## Data availability statement

The original contributions presented in the study are included in the article/Supplementary Material. Further inquiries can be directed to the corresponding author.

## Ethics statement

Since all KIRC data were obtained from the TCGA and GEO databases, ethical approval and informed consent were not required.

## Author contributions

All authors contributed to the study's conception and design. Conceptualization, methodology, data curation, formal analysis, visualization, and writing-original draft preparation were performed by XS. Supervision, writing-reviewing, and editing were performed by PL. All authors contributed to the article and approved the submitted version.

## References

- Hsieh JJ, Purdue MP, Signoretti S, Swanton C, Albiges L, Schmidinger M, et al. Renal cell carcinoma. *Nat Rev Dis Primers* (2017) 3:17009. doi: 10.1038/nrdp.2017.9
- Capitanio U, Bensalah K, Bex A, Boorjian SA, Bray F, Coleman J, et al. Epidemiology of renal cell carcinoma. *Eur Urol* (2019) 75(1):74–84. doi: 10.1016/j.eururo.2018.08.036
- Siegel RL, Miller KD, Fuchs HE, Jemal A. Cancer Statistics, 2021. *CA Cancer J Clin* (2021) 71(1):7–33. doi: 10.3322/caac.21654
- Atkins MB, Tannir NM. Current and emerging therapies for first-line treatment of metastatic clear cell renal cell carcinoma. *Cancer Treat Rev* (2018) 70:127–37. doi: 10.1016/j.ctrv.2018.07.009
- Powles T, Albiges L, Bex A, Grunwald V, Porta C, Procopio G, et al. E.G.C.E.A. clinical guidelines atesmo.org, ESMO clinical practice guideline update on the use of immunotherapy in early stage and advanced renal cell carcinoma. *Ann Oncol* (2021) 32(12):1511–9. doi: 10.1016/j.annonc.2021.09.014
- Makhov P, Joshi S, Ghatalia P, Kutikov A, Uzzo RG, Kolenko VM. Resistance to systemic therapies in clear cell renal cell carcinoma: Mechanisms and management strategies. *Mol Cancer Ther* (2018) 17(7):1355–64. doi: 10.1158/1535-7163.MCT-17-1299
- Krokeide SZ, Laerdahl JK, Salah M, Luna L, Cederkvist FH, Fleming AM, et al. Human NEIL3 is mainly a monofunctional DNA glycosylase removing spiroimidiohydantoin and guanidinohydantoin. *DNA Repair (Amst)* (2013) 12(12):1159–64. doi: 10.1016/j.dnarep.2013.04.026
- Liu M, Bandaru V, Bond JP, Jaruga P, Zhao X, Christov PP, et al. The mouse ortholog of NEIL3 is a functional DNA glycosylase *in vitro* and *in vivo*. *Proc Natl Acad Sci U.S.A.* (2010) 107(11):4925–30. doi: 10.1073/pnas.0908307107
- Zhou J, Chan J, Lambele M, Yusufzai T, Stumpf J, Opreko PL, et al. NEIL3 repairs telomere damage during S phase to secure chromosome segregation at mitosis. *Cell Rep* (2017) 20(9):2044–56. doi: 10.1016/j.celrep.2017.08.020
- Massaad MJ, Zhou J, Tsuchimoto D, Chou J, Jabara H, Janssen E, et al. Deficiency of base excision repair enzyme NEIL3 drives increased predisposition to autoimmunity. *J Clin Invest* (2016) 126(11):4219–36. doi: 10.1172/JCI85647
- Zhao Z, Gad H, Benitez-Buelga C, Sanjiv K, Xiangwei H, Kang H, et al. NEIL3 prevents senescence in hepatocellular carcinoma by repairing oxidative lesions at telomeres during mitosis. *Cancer Res* (2021) 81(15):4079–93. doi: 10.1158/0008-5472.CAN-20-1028
- Kauffmann A, Rosselli F, Lazar V, Winnepenninckx V, Mansuet-Lupo A, Dessen P, et al. High expression of DNA repair pathways is associated with metastasis in melanoma patients. *Oncogene* (2008) 27(5):565–73. doi: 10.1038/sj.onc.1210700
- de Sousa JF, Torrieri R, Serafim RB, Di Cristofaro LF, Escanfella FD, Ribeiro R, et al. Expression signatures of DNA repair genes correlate with survival prognosis of astrocytoma patients. *Tumour Biol* (2017) 39(4):1010428317694552. doi: 10.1177/1010428317694552
- Liu XS, Li B, Chen Q, Li J, Cohen D, Zeng Z, et al. TIMER2.0 for analysis of tumor-infiltrating immune cells. *Nucleic Acids Res* (2020) 48(W1):W509–14. doi: 10.1093/nar/gkaa407
- Cline MS, Craft B, Swatloski T, Goldman M, Ma S, Haussler D, et al. Exploring TCGA pan-cancer data at the UCSC cancer genomics browser. *Sci Rep* (2013) 3:2652. doi: 10.1038/srep02652
- Chen W, Lin W, Wu L, Xu A, Liu C, Huang P. A novel prognostic predictor of immune microenvironment and therapeutic response in kidney renal clear cell carcinoma

## Funding

This work was supported by the National Natural Science Foundation of China (J2024008).

## Acknowledgments

We acknowledge the TIMER, TCGA, GEO, GEPIA, and TISIDB databases for free use.

## Conflict of interest

The authors declare that the research was conducted in the absence of any commercial or financial relationships that could be construed as a potential conflict of interest.

## Publisher's note

All claims expressed in this article are solely those of the authors and do not necessarily represent those of their affiliated organizations, or those of the publisher, the editors and the reviewers. Any product that may be evaluated in this article, or claim that may be made by its manufacturer, is not guaranteed or endorsed by the publisher.

## Supplementary material

The Supplementary Material for this article can be found online at: <https://www.frontiersin.org/articles/10.3389/fonc.2023.1073941/full#supplementary-material>

- based on necroptosis-related gene signature. *Int J Med Sci* (2022) 19(2):377–92. doi: 10.7150/ijms.69060
17. Wang L, Liu XX, Yang YM, Wang Y, Song YY, Gao S, et al. RHBDF2 gene functions are correlated to facilitated renal clear cell carcinoma progression. *Cancer Cell* (2021) 21(1):590. doi: 10.1186/s12935-021-02277-0
18. Barrett T, Troup DB, Wilhite SE, Ledoux P, Rudnev D, Evangelista C, et al. NCBI GEO: archive for high-throughput functional genomic data. *Nucleic Acids Res* (2009) 37 (Database issue):D885–90. doi: 10.1093/nar/gkn764
19. Liu J, Lichtenberg T, Hoadley KA, Poisson LM, Lazar AJ, Cherniack AD, et al. An integrated TCGA pan-cancer clinical data resource to drive high-quality survival outcome analytics. *Cell* (2018) 173(2):400–416.e11. doi: 10.1016/j.cell.2018.02.052
20. Yu G, Wang LG, Han Y, He QY. clusterProfiler: An R package for comparing biological themes among gene clusters. *OMICS* (2012) 16(5):284–7. doi: 10.1089/omi.2011.0118
21. Subramanian A, Tamayo P, Mootha VK, Mukherjee S, Ebert BL, Gillette MA, et al. Gene set enrichment analysis: A knowledge-based approach for interpreting genome-wide expression profiles. *Proc Natl Acad Sci U.S.A.* (2005) 102(43):15545–50. doi: 10.1073/pnas.0506580102
22. Tang Z, Li C, Kang B, Gao G, Li C, Zhang Z. GEPIA: A web server for cancer and normal gene expression profiling and interactive analyses. *Nucleic Acids Res* (2017) 45 (W1):W98–W102. doi: 10.1093/nar/gkx247
23. Szklarczyk D, Gable AL, Nastou KC, Lyon D, Kirsch R, Pyysalo S, et al. The STRING database in 2021: customizable protein-protein networks, and functional characterization of user-uploaded gene/measurement sets. *Nucleic Acids Res* (2021) 49 (D1):D605–12. doi: 10.1093/nar/gkaa1074
24. Liu CJ, Hu FF, Xia MX, Han L, Zhang Q, Guo AY. GSCALite: A web server for gene set cancer analysis. *Bioinformatics* (2018) 34(21):3771–2. doi: 10.1093/bioinformatics/bty411
25. Chen B, Khodadoust MS, Liu CL, Newman AM, Alizadeh AA. Profiling tumor infiltrating immune cells with CIBERSORT. *Methods Mol Biol* (2018) 1711:243–59. doi: 10.1007/978-1-4939-7493-1\_12
26. Bindea G, Mlecnik B, Tosolini M, Kirilovsky A, Waldner M, Obenauf AC, et al. Spatiotemporal dynamics of intratumoral immune cells reveal the immune landscape in human cancer. *Immunity* (2013) 39(4):782–95. doi: 10.1016/j.immuni.2013.10.003
27. Ru B, Wong CN, Tong Y, Zhong JY, Zhong SSW, Wu WC, et al. TISIDB: An integrated repository portal for tumor-immune system interactions. *Bioinformatics* (2019) 35(20):4200–2. doi: 10.1093/bioinformatics/btz210
28. Dawson MA, Kouzarides T. Cancer epigenetics: From mechanism to therapy. *Cell* (2012) 150(1):12–27. doi: 10.1016/j.cell.2012.06.013
29. Kulis M, Esteller M. DNA Methylation and cancer. *Adv Genet* (2010) 70:27–56. doi: 10.1016/B978-0-12-380866-0.60002-2
30. Zhao C, Liu J, Zhou H, Qian X, Sun H, Chen X, et al. NEIL3 may act as a potential prognostic biomarker for lung adenocarcinoma. *Cancer Cell Int* (2021) 21(1):228. doi: 10.1186/s12935-021-01938-4
31. Hao X, Luo H, Krawczyk M, Wei W, Wang W, Wang J, et al. DNA Methylation markers for diagnosis and prognosis of common cancers. *Proc Natl Acad Sci U.S.A.* (2017) 114(28):7414–9. doi: 10.1073/pnas.1703577114
32. Ullah M, Aoudjehout W, Pimpie C, Pocard M, Mirshahi M. Mitosis in cancer cell increases immune resistance via high expression of HLA-G and PD-L1. *Cancers (Basel)* (2020) 12(9):2661. doi: 10.3390/cancers12092661
33. Zhao H, Wu L, Yan G, Chen Y, Zhou M, Wu Y, et al. Inflammation and tumor progression: Signaling pathways and targeted intervention. *Signal Transduct Target Ther* (2021) 6(1):263. doi: 10.1038/s41392-021-00658-5
34. Koritala BSC, Porter KI, Arshad OA, Gajula RP, Mitchell HD, Arman T, et al. Night shift schedule causes circadian dysregulation of DNA repair genes and elevated DNA damage in humans. *J Pineal Res* (2021) 70(3):e12726. doi: 10.1111/jpi.12726
35. Slade D. PARP and PARG inhibitors in cancer treatment. *Genes Dev* (2020) 34(5-6):360–94. doi: 10.1101/gad.334516.119
36. Ghosh M, Saha S, Bettke J, Nagar R, Parrales A, Iwakuma T, et al. Mutant p53 suppresses innate immune signaling to promote tumorigenesis. *Cancer Cell* (2021) 39 (4):494–508.e5. doi: 10.1016/j.ccell.2021.01.003
37. McGranahan N, Rosenthal R, Hiley CT, Rowan AJ, Watkins TBK, Wilson GA, et al. Allele-specific HLA loss and immune escape in lung cancer evolution. *Cell* (2017) 171(6):1259–1271.e11. doi: 10.1016/j.cell.2017.10.001
38. Barrueto L, Caminero F, Cash L, Makris C, Lamichane P, Deshmukh RR. Resistance to checkpoint inhibition in cancer immunotherapy. *Transl Oncol* (2020) 13 (3):100738. doi: 10.1016/j.tranon.2019.12.010
39. Zaretsky JM, Garcia-Diaz A, Shin DS, Escuin-Ordinas H, Hugo W, Hu-Lieskovan S, et al. Mutations associated with acquired resistance to PD-1 blockade in melanoma. *N Engl J Med* (2016) 375(9):819–29. doi: 10.1056/NEJMoa1604958
40. Wan B, Huang Y, Liu B, Lu L, Lv C. AURKB: A promising biomarker in clear cell renal cell carcinoma. *PeerJ* (2019) 7:e7718. doi: 10.7717/peerj.7718
41. de Miranda NF, Bjorkman A, Pan-Hammarstrom Q. DNA Repair: The link between primary immunodeficiency and cancer. *Ann N Y Acad Sci* (2011) 1246:50–63. doi: 10.1111/j.1749-6632.2011.06322.x
42. Vuong L, Kotecha RR, Voss MH, Hakimi AA. Tumor microenvironment dynamics in clear-cell renal cell carcinoma. *Cancer Discovery* (2019) 9(10):1349–57. doi: 10.1158/2159-8290.CD-19-0499
43. Zhang S, Zhang E, Long J, Hu Z, Peng J, Liu L, et al. Immune infiltration in renal cell carcinoma. *Cancer Sci* (2019) 110(5):1564–72. doi: 10.1111/cas.13996
44. Hinshaw DC, Shevde LA. The tumor microenvironment innately modulates cancer progression. *Cancer Res* (2019) 79(18):4557–66. doi: 10.1158/0008-5472.CAN-18-3962
45. Mier JW. The tumor microenvironment in renal cell cancer. *Curr Opin Oncol* (2019) 31(3):194–9. doi: 10.1097/CCO.0000000000000512
46. Dai S, Zeng H, Liu Z, Jin K, Jiang W, Wang Z, et al. Intratumoral CXCL13(+)/CD8(+) T cell infiltration determines poor clinical outcomes and immunoevasive contexture in patients with clear cell renal cell carcinoma. *J Immunother Cancer* (2021) 9(2):e001823. doi: 10.1136/jitc-2020-001823
47. Qi Y, Xia Y, Lin Z, Qu Y, Qi Y, Chen Y, et al. Tumor-infiltrating CD39(+)/CD8(+) T cells determine poor prognosis and immune evasion in clear cell renal cell carcinoma patients. *Cancer Immunol Immunother* (2020) 69(8):1565–76. doi: 10.1007/s00262-020-02563-2
48. Senbabaoglu Y, Gejman RS, Winer AG, Liu M, Van Allen EM, de Velasco G, et al. Tumor immune microenvironment characterization in clear cell renal cell carcinoma identifies prognostic and immunotherapeutically relevant messenger RNA signatures. *Genome Biol* (2016) 17(1):231. doi: 10.1186/s13059-016-1092-z
49. Yang F, Zhao J, Luo X, Li T, Wang Z, Wei Q, et al. Transcriptome profiling reveals b-lineage cells contribute to the poor prognosis and metastasis of clear cell renal cell carcinoma. *Front Oncol* (2021) 11:731896. doi: 10.3389/fonc.2021.731896
50. Lin A, Schildknecht A, Nguyen LT, Ohashi PS. Dendritic cells integrate signals from the tumor microenvironment to modulate immunity and tumor growth. *Immunol Lett* (2010) 127(2):77–84. doi: 10.1016/j.imlet.2009.09.003
51. Law AMK, Valdes-Mora F, Gallego-Ortega D. Myeloid-derived suppressor cells as a therapeutic target for cancer. *Cells* (2020) 9(3):561. doi: 10.3390/cells9030561
52. Zhang S, Ma X, Zhu C, Liu L, Wang G, Yuan X. The role of myeloid-derived suppressor cells in patients with solid tumors: A meta-analysis. *PLoS One* (2016) 11(10):e0164514. doi: 10.1371/journal.pone.0164514
53. Andrews LP, Marciscano AE, Drake CG, Vignali DA. LAG3 (CD223) as a cancer immunotherapy target. *Immunol Rev* (2017) 276(1):80–96. doi: 10.1111/imr.12519
54. Sawant DV, Yano H, Chikina M, Zhang Q, Liao M, Liu C, et al. Adaptive plasticity of IL-10(+) and IL-35(+) Treg cells cooperatively promotes tumor T cell exhaustion. *Nat Immunol* (2019) 20(6):724–35. doi: 10.1038/s41590-019-0346-9
55. Mannino MH, Zhu Z, Xiao H, Bai Q, Wakefield MR, Fang Y. The paradoxical role of IL-10 in immunity and cancer. *Cancer Lett* (2015) 367(2):103–7. doi: 10.1016/j.canlet.2015.07.009